Relative-Intensity-Noise Cancellation in Bandpass External-Modulation Links

Roger Helkey, *Member, IEEE*

***Abstract*— A new method of optically summing time-shifted complementary signals to cancel relative intensity noise (RIN) in narrow-band extbernal-modulation optical links is proposed and demonstrated. Differential-link noise figure and dynamic-range improvement are compared to the conventional low-biased modulator configuration for suboctave applications. RIN suppression of 12 dB at 4 GHz is demonstrated.**

***Index Terms*—Laser noise, optical communication, optical-fiber applications, optical modulation, optical noise.**

I. Introduction

ANALOG optical links are important for transmission of signals over long distances due to the low loss of optical fiber. The major application of optical links has been for cable television (CATV) signal distribution, which requires broad-band signal transmission. High-performance applications have used external modulation of an expensive Nd : YAG laser with low intensity noise, as shown in Fig. 1(a). More recent applications such as cellular radio and personal communications system (PCS) base-station signal transmission [1] and antenna remoting [2] are narrow-band, and are considerably more cost sensitive. An externally modulated Nd : YAG laser is not a cost-effective solution, but low-cost semiconductor lasers have intensity noise that is too high for many applications.

The link degradation due to laser intensity noise can be reduced with a conventional laser noise-suppression method of differential detection [3]–[5] using two outputs of an external modulator with equal optical path delays, as shown in Fig. 1(b) [6], [7]. The two outputs from the Mach–Zehnder interferometer are out of phase, so subtracting them with a differential detector sums the signal component while canceling the common-mode laser intensity noise. For broad-band applications such as CATV, the differential detection method can suppress relative intensity noise (RIN) over the modulation bandwidth, as long as the path length from each output is carefully matched to a small fraction of the electrical wavelength. This critical length matching between fibers can be difficult when installing a link over a long distance. Although this technique allows a lower cost semiconductor laser to be used for the source, the requirement for a second fiber precisely length matched to the first fiber substantially increases the system cost. For applications with greater than an octave bandwidth, the link needs to have low second-order distortion and a conventional Mach–Zehnder modulator must be biased at quadrature.

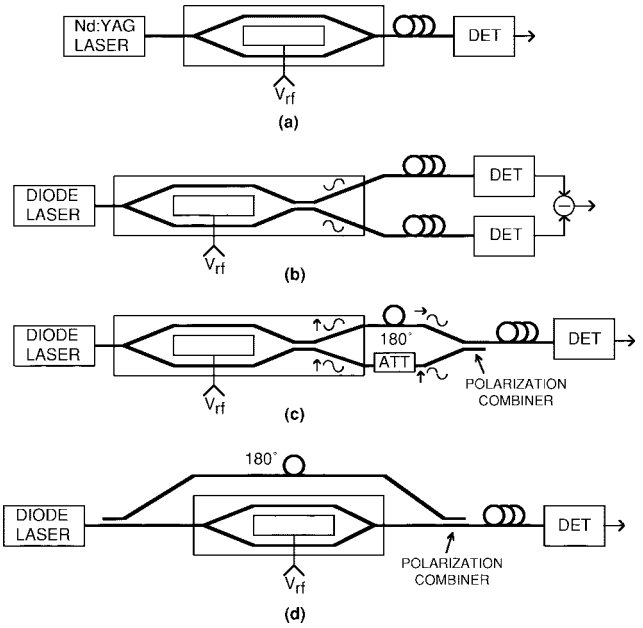

Fig. 1. Block diagram of (a) external-modulation link, (b) conventional differential intensity-noise cancellation configuration, (c) experimental delayed-differential intensity-noise cancellation configuration, and (d) alternate delayed-differential implementation.

Here, a new bandpass differential method, shown in Fig. 1(c), is proposed and demonstrated. This method has the same benefit of intensity noise cancellation of the previous differential detection method, but is effective only over a suboctave RF bandwidth. The two complementary output signals of the modulator are subtracted by delaying one output by half of the modulation period and then optically summing the signals *incoherently* in a polarization coupler. This incoherent summing uses polarization-maintaining fiber from the modulator output to the polarization coupler. Length matching is not required on the scale of an optical wavelength because of the incoherent summing. In order to provide the correct modulation phases at the desired center frequency, these short fiber paths to the polarization coupler still have length tolerances similar to that required for the equal-delay differential method, but are matched over a much shorter length of fiber. However, unlike the conventional differential output configuration, this method uses only one long single-mode fiber from the output of the polarization coupler to the detector, so no length matching is required after the polarization coupler.

Manuscript received December 3, 1997; revised May 7, 1998. This work was supported under Air Force Contract F19628-95-C-002.

The author is with the MIT Lincoln Laboratory, Lexington, MA 02173 USA.

Publisher Item Identifier S 0018-9480(98)09036-X.

This technique of incoherently summing delayed signals can also be applied to unmodulated light. Another implementation for an external-modulation link would be summing a delayed portion of the optical power from before the modulator, as shown in Fig. 1(d). This technique would also cancel optical intensity noise, but would not have the advantage of using both modulator outputs to enhance the signal. The polarization-combining technique demonstrated here can only be used if there are no polarization-sensitive components further in the link.

Here, the performance of the delayed differential configuration is compared to a conventional low-biased link to examine which technique is more effective for narrow-band links. Closed-form solutions are given for gain, noise figure, and dynamic range of low-biased and delayed differential links.

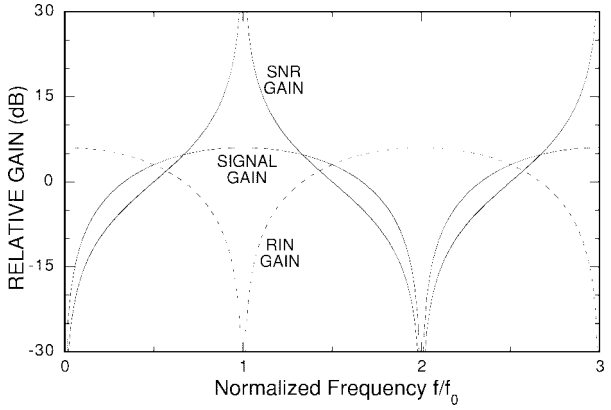

Fig. 2. Signal gain, noise gain, and SNR gain as a function of normalized frequency.

II. Delayed Differential Link

The amount of intensity noise cancellation using differential detection is limited by the relative amplitude and phase imbalance of the modulator outputs. In principle, a differential external-modulation link can completely cancel the RIN of the laser source. Using the delayed differential configuration, shown in Fig. 1(c), the amount of intensity noise cancellation is limited even for perfect amplitude balance because the noise components are exactly out of phase at only a single frequency. For moderate bandwidth systems, the dominant error would be phase imbalance due to the frequency-dependent phase of the delay line.

The output intensity noise of a differential link with one output delayed by a time τ can be calculated by summing the output intensity noise $n(t)$ of a single-ended link with the same delayed output $n(t-\tau)$. The resulting ratio of RIN power for a delayed differential link compared to a single-ended link can be given as a noise gain term G_n

$$G_n = 4\cos^2\left(\frac{\pi f}{2f_o}\right) \tag{1}$$

where f is the noise frequency and f_o is the center frequency at which the delay-line electrical phase shift is 180°. At low frequency, the noise terms are in phase, and the delayed differential RIN power increases by a factor of four compared to a single-output link due to the increase in optical power.

The reduction in intensity noise from a differential configuration can be related to an apparent reduction in laser RIN for an equivalent single-ended link. The RIN power spectral density $\overline{N}_{\rm RIN}$ referenced to the link output is [8]

$$\overline{N}_{\rm RIN} \equiv {\rm RIN}\, I_d^2 R_d \tag{2}$$

where RIN is the RIN parameter of the laser, I_d is the average photodetector current, and R_d is the photodetector load impedance. The factor of four increase in low-frequency noise power in the differential link is accompanied by doubling of the photodetector current, so there is no difference at low frequency between the apparent RIN measured using the delayed differential link and the actual laser RIN. Due to the doubled photocurrent, the change in effective RIN $G_{\rm RIN}$ for the delayed differential method is equal to one-quarter of G_n

$$G_{\rm RIN} = \cos^2\left(\frac{\pi f}{2f_o}\right). \tag{3}$$

$G_{\rm RIN}$ gives the apparent change in laser RIN when measuring the intensity noise at the output of a differential link, and is equal to zero for perfect RIN cancellation and equal to one for noise components that add in-phase. If the maximum frequency range over which a given RIN suppression can be achieved is given by $f = f_o \pm \Delta f$, then

$$\Delta f = \frac{2f_o}{\pi}\sin^{-1}\left(\sqrt{G_{\rm RIN}}\right). \tag{4}$$

The relative bandwidth is given by

$${\rm BW} \equiv \frac{2\Delta f}{f_o} \cong \frac{4\sqrt{G_{\rm RIN}}}{\pi}. \tag{5}$$

Noise cancellation of $G_{\rm RIN} = -20$ dB can be achieved over a relative bandwidth of ~13%.

The calculations in Fig. 2 show that RIN can be suppressed arbitrarily well at a single frequency for the ideal case of perfect amplitude balance and incoherent signal addition. The reduction in delayed differential-link noise figure would be approximately equal to this reduction in effective RIN as long as the differential link remains RIN limited and the modulator-bias point is the same for both cases. However, the improvement in link noise figure and dynamic range of a differential link compared to a single-output link depends on a number of link parameters. When the laser RIN is sufficiently suppressed, the link noise figure will be dominated by input thermal noise, shot noise, or noise from the amplifier following the photodetector. In addition, the following two sections will show that, for suboctave links, the optimum modulator-bias point is different for the single output and differential configurations.

III. Low-Biased Modulator

A common approach to substantially reducing the effect of laser RIN in narrow bandwidth external-modulation links has been to bias the modulator for low optical transmission [9]–[11]. Low modulator bias reduces the output noise contribution of shot noise and laser RIN faster than the output signal

level, resulting in an improvement in the signal-to-noise (SNR) ratio at the expense of reduced link gain. Low modulator bias increases second-order intermodulation products, but these fall out of band for suboctave links.

The shot-noise power spectral density $\overline{N}_{\rm shot}$ referenced to the link output is [8]

$$\overline{N}_{\rm shot} \equiv 2qI_dR_d \tag{6}$$

where q is the electron charge, I_d is the detector current, and R_d is the detector load impedance. The postamplifier-noise power spectral density $\overline{N}_{\rm amp}$ referenced to the link output is

$$\overline{N}_{\rm amp} \equiv F_akT \tag{7}$$

where F_a is the noise figure of the receiver chain following the photodetector, k is the Boltzman's constant, and T is the temperature. It is important to include this effect of receiver noise figure when optimizing the bias point of the modulator.

The noise power spectral density due to thermal noise at the modulator input is the product kT for an impedance-matched traveling-wave modulator. This thermal noise contribution increases by a factor of two for an impedance-matched lumped-element modulator where the modulator internal resistance generates noise [12], and at low frequency for a traveling-wave modulator where the noise from the termination resistor also couples to the optical wave [13]. The effect of input thermal noise is small for broad-band modulators and will be neglected in most of the analysis here.

In order to avoid degrading link performance, the laser RIN power should be kept much lower than the sum of the shot noise and receiver noise [13]. This condition is met if

$$\text{RIN} \ll \frac{2q}{I_d} + \frac{F_akT}{I_d^2R_d} \tag{8}$$

so that the increase in noise figure due to RIN is much less than 3 dB.

A shot-noise limited link with a detector current $I_d = 1$ mA requires a laser RIN of much less than -155 dB $\cdot$ Hz^{-1}, which is achievable with current diode laser technology. Each factor of an increase of ten in the detector current requires a reduction of 10 dB in the RIN to avoid degrading the link noise figure. Shot-noise limited operation with a detector current of 10 mA requires laser RIN much less than -165 dB $\cdot$ Hz^{-1}. The shot-noise-limit condition given in (8) can be used directly if I_d is already determined, e.g., for broad-band links where the modulator is biased at quadrature. However, the necessary laser RIN to avoid degrading narrow-band links is not adequately specified by this equation, as the photodetector current is not an independent variable, but is optimized through the modulator-bias angle based on other link parameters. The detector photocurrent I_d as a function of the modulator-bias angle θ is

$$I_d = I_q(1 + \cos\,\theta) \tag{9}$$

where I_q is the detector current with the modulator at quadrature bias ($\theta = 90°$).

The single-output link gain G_1 is

$$G_1 = \left(\frac{\pi I_q \sin\,\theta}{V_\pi}\right)^2 R_sR_d \tag{10}$$

where R_s is the source resistance and V_π is the modulator half-wave RF switching voltage measured at the modulator input. This value of V_π includes the effect of impedance mismatch and any modulator impedance matching. Consequently, the RF value of V_π can be considerably lower than the dc value for a lumped-element modulator with impedance matching, or higher than the dc value for a modulator with a velocity mismatch between the electrical and optical wave or an electrode impedance which is lower than 50 Ω.

Optimum link performance is obtained by increasing the optical power until shot noise dominates over the noise of the post-detector amplifier, and by using a laser with low RIN. Consequently, the performance of single-output and differential links will be compared to the shot-noise contribution of an identical single-output link. This comparison is useful in that the relative effect of modulator-bias point and of differential outputs can be characterized for many links by only one or two parameters.

The noise figure F_1 for a single output traveling-wave modulator biased at an angle θ is

$$F_1 = 1 + F_{q,\,\rm shot}\left(\frac{1 + \cos\,\theta + p_{\rm amp} + p_{\rm RIN}(1 + \cos\,\theta)^2}{\sin^2\,\theta}\right) \tag{11}$$

where the first term is the thermal noise contribution for a traveling-wave modulator. $F_{q,\,\rm shot}$ is the contribution of shot noise for a single-output link with the modulator at quadrature bias

$$F_{q,\,\rm shot} \equiv \frac{2qV_\pi^2}{\pi^2kTR_sI_q} \cong \frac{V_\pi^2(162.2\ \text{mA} \cdot V^{-2})}{I_q} \tag{12}$$

where the numerical value is calculated at room temperature for $R_s = 50\ \Omega$.

The ratio of the equivalent-input amplifier-noise power to the shot-noise power at quadrature $p_{\rm amp}$ is given by

$$p_{\rm amp} \equiv \frac{F_akT}{2qI_qR_d} \cong \frac{0.4\ \text{mA}}{I_q} \tag{13}$$

where the numerical value is calculated at room temperature for $F_a = 2$ dB and $R_d = 50\ \Omega$. Under these conditions, shot noise is higher than amplifier noise for a detector current $I_d > 0.4$ mA. This relationship is not dependent on the modulator-bias point and also holds for direct modulation links. The relative amplifier-noise contribution $p_{\rm amp}$ can be reduced substantially by using detector impedance matching to increase R_d. The ratio of the RIN noise power to the shot-noise power at quadrature bias $p_{\rm RIN}$ is given by

$$p_{\rm RIN} \equiv \frac{I_q\text{RIN}}{2q} \cong \frac{I_q\text{RIN}}{-155\ \text{dB} \cdot \text{Hz}^{-1} \cdot \text{mA}}. \tag{14}$$

For broad-band links, which must be biased at quadrature, $F_1 \cong F_{q,\,\rm shot}$ in the high V_π limit if laser intensity noise is small ($p_{\rm RIN} \ll 1$) and the optical power is high ($p_{\rm amp} \ll 1$). For large $p_{\rm RIN}$, the resulting RIN-limited noise figure at quadrature bias is approximately $p_{\rm RIN} * F_{q,\,\rm shot}$.

The bias angle for optimum noise figure of a narrow-band link does not depend on the input thermal noise term. The noise figure of a single-output link is shown in Fig. 3(a) as a function

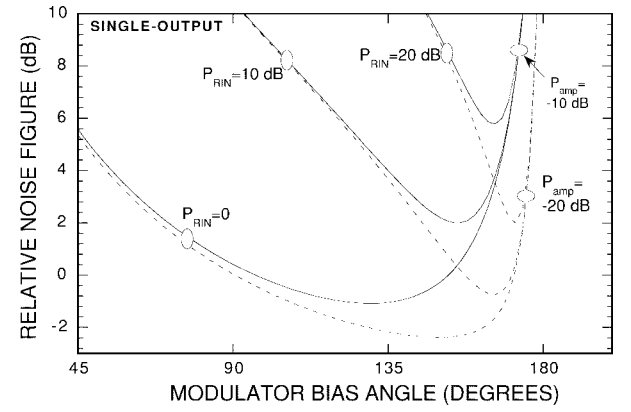

(a)

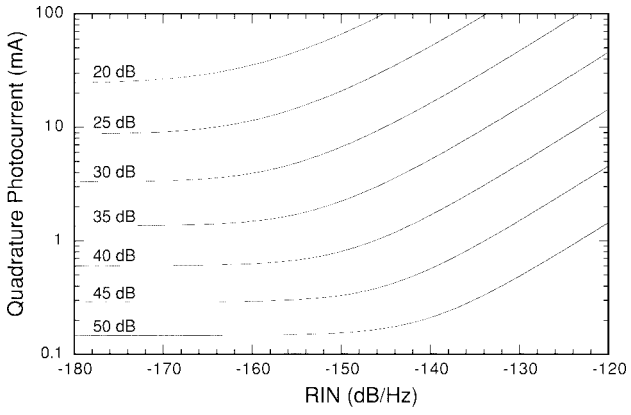

(b)

Fig. 3. (a) Optimum noise figure of a single-output link relative to the shot-noise limit at quadrature as a function of modulator bias-angle using normalized parameters. These results are valid in the high V_π limit where noise figure $\gg$3 dB. (b) Noise figure of a single-output link as a function of RIN and photocurrent for $V_\pi = 5$ V, $R_s = 50\ \Omega$, $R_d = 50\ \Omega$, $F_a = 2$ dB.

of modulator-bias angle, relative to the noise figure in the shot-noise limit at quadrature bias. This relative noise figure can be characterized by the two parameters $p_{\rm amp}$ and $p_{\rm RIN}$ because most present modulators operate in the high V_π limit where input thermal noise can be neglected ($F_{q,\,\rm shot} \gg 1$). The optimum noise figure is plotted in Fig. 3(b) for the case of $R_s = 50\ \Omega$, $R_d = 50\ \Omega$, $V_\pi = 5$ V, and a receiver noise figure of 2 dB. An approximate solution to the optimum noise figure $F_{\rm opt1}$ of a narrow-band link that is valid over a wide range of $p_{\rm amp}$ and $p_{\rm RIN}$ is

$$F_{\rm opt1} \cong 1 + F_{q,\,\rm shot} \cdot\left(\frac{1}{2} + \frac{p_{\rm amp}}{2} + \sqrt{p_{\rm RIN}p_{\rm amp} + \frac{p_{\rm amp}}{2} + \left(\frac{p_{\rm amp}}{2}\right)^2}\right). \quad (15)$$

For sufficiently large $p_{\rm amp}$, the optimum bias is at quadrature and there is no improvement by low-biasing the modulator. For small $p_{\rm amp}$, (15) simplifies to

$$F_{\rm opt1} \cong 1 + F_{q,\,\rm shot}\left(\frac{1}{2} + \sqrt{p_{\rm amp}}\sqrt{p_{\rm RIN} + \frac{1}{2}}\right). \quad (16)$$

If $p_{\rm RIN}$ is also small, then $F_{\rm opt1} \cong F_{q,\,\rm shot}/2$, an improvement over quadrature bias of 3 dB, which agrees with previous results [9].

For sufficiently large $P_{\rm RIN}$, both (15) and (16) reduce to the RIN-limited low-bias noise figure $F_{\rm opt1,RIN}$

$$F_{\rm opt1,\,RIN} \cong \sqrt{p_{\rm amp}p_{\rm RIN}}F_{q,\,\rm shot} \quad (17)$$

so the noise figure rises more slowly with increasing laser RIN than quadrature biased links. High RIN low-biased links have a noise figure proportional to the square root of the laser RIN and inversely proportional to the laser optical power. In contrast, RIN-limited quadrature biased links have a noise figure that is proportional to the RIN and independent of optical power.

When the modulator is biased for optimum noise figure, the gain $G_{\rm opt1}$ for small $p_{\rm amp}$ is approximately

$$G_{\rm opt1} \cong \sqrt{\frac{p_{\rm amp}}{p_{\rm amp} + p_{\rm RIN}/4 + 1/8}}\left(\frac{\pi I_q}{V_\pi}\right)^2 R_s R_d. \quad (18)$$

Shot-noise limited operation requires that the increase in noise figure due to laser RIN be much less than 3 dB. This condition can be found directly from the approximate noise-figure solution of (15), which results in a fairly complex expression. A simpler expression, which is accurate over most common-link parameters, is

$$\rm RIN \ll \frac{3q^2R_d}{2F_akT} + \frac{10q}{I_q} + \frac{2F_akT}{I_q^2R_d}. \quad (19)$$

For very small I_q, this RIN limit is a factor of two higher than the quadrature-bias limit given in (8). The increase in allowable laser RIN for low modulator bias is even larger at higher photocurrent. The most important difference between this expression and the quadrature-biased RIN limit given in (8) is the first term that is independent of optical power. The value of this constant term in (19) is $-$155 dB/Hz for a 50-Ω detector impedance and a receiver noise figure of 2 dB. The actual RIN limit begins to increase at very high optical power, but this effect can be neglected for typical link parameter values and is not included in (19).

Analytic expressions for the dynamic range can be calculated by a power series expansion of the modulator transfer function. For the single-output modulator, the spurious-free dynamic range $\rm SFDR_1$ due to third-order distortion products is given by the power ratio

$$\rm SFDR_1 = \left(\frac{F_{q,\,shot}}{F_1}\right)^{2/3} SFDR_{q,\,shot} \quad (20)$$

where $\rm SFDR_{q,\,shot}$ is the shot-noise limited dynamic range for the modulator biased at quadrature [14]

$$\rm SFDR_{q,\,shot} = \left(\frac{2I_q}{qB}\right)^{2/3} \quad (21)$$

and B is the bandwidth in which the spur-free dynamic range is measured. Third-order spur-free dynamic range is the input power range for a two-tone input signal where each of the tones are above the noise floor and each of the third-order intermodulation products are below the noise floor. In previous work, the dynamic range has been expressed as a voltage ratio, in which case, the exponent in (21) would be one-third [14], [15] rather than two-thirds. The dynamic range in (20) can be expanded, as shown in (22) at the bottom of the following

page, where $p_{\rm mod}$ is the ratio of the input thermal noise power to the shot-noise power for a single-output traveling-wave modulator biased at quadrature

$$p_{\rm mod} \equiv \frac{1}{F_{q,\,\rm shot}} \tag{23}$$

but is negligible for broad-band modulators with high V_π. Even for cases that are shot-noise limited at quadrature, amplifier noise contributes at the optimum low bias for narrow-band links. Using the noise figure approximation of (16) and neglecting $p_{\rm mod}$, for small $p_{\rm amp}$, the optimum dynamic range $\rm SFDR_{opt1}$ in the high V_π limit is

$$\rm SFDR_{opt1} \cong \left(\frac{4I_q}{qB\left(1+2\sqrt{p_{\rm amp}}\sqrt{p_{\rm RIN}+1/2}\right)} \right)^{2/3} \tag{24}$$

which is approximately 2 dB higher than for a shot-noise-limited link at quadrature bias [10] if $p_{\rm RIN}$ and $p_{\rm amp}$ are small. The 2-dB increase in dynamic range comes from the 3-dB decrease in link noise, not from improved link linearity.

IV. Low-Biased Differential Link

Previous demonstrations of differential links have used the modulator biased at quadrature in order to give low second-order distortion for broad-band applications. Here, the use of low-biased differential detection links is proposed and the resulting performance is analyzed. The differential RIN cancellation technique can still be used with unequal power outputs from the modulator if the RIN amplitudes of the two outputs are adjusted to be equal before subtracting the two signals. This same technique of equalizing the RIN amplitudes before subtraction can be used for other modulator topologies. Linearized modulators [16], [17] and directional coupler modulators [18] can have complementary outputs. A fraction of the input optical power can also be used for differential operation of single-output modulators. Differential operation with low modulator bias has an advantage for links that are detector current limited, as the average detector current can be substantially reduced.

The relative RIN amplitudes can be adjusted by optically attenuating the higher power signal, or by providing a different electrical gain after each photodetector. A simple method of adjusting the relative levels electrically is to use impedance matching to give a different load impedance to each photodetector. The electrical gain method of RIN balancing has the advantage of higher link performance, as optical attenuation increases the relative effect of shot noise. However, only the optical attenuation method can be used with the single-fiber differential delay configuration, so only this configuration will be analyzed here.

In this case, the differential-link gain G_2 of the dual output modulator biased at an angle θ is

$$G_2 = \left(\frac{2\pi I_q \sin\theta}{V_\pi(1+|\cos\theta|)} \right)^2 R_s R_d. \tag{25}$$

The differential-link noise figure F_2 with the higher optical power output optically attenuated to cancel the RIN contribution is

$$F_2 = 1 + F_{q,\,\rm shot}\left(\frac{1+|\cos\theta|}{2} + \frac{p_{\rm amp}}{4}\frac{1+|\cos\theta|}{1-|\cos\theta|} + G_{\rm RIN}p_{\rm RIN}\sin^2\theta \right) \tag{26}$$

where the shot noise $F_{q,\,\rm shot}$, the amplifier noise $p_{\rm amp}$, and the RIN parameter $p_{\rm RIN}$ are the values for an equivalent single-output link in order to directly compare the performance of single-output and differential links. This expression assumes that the photodetectors are not impedance matched for maximum gain, so that the detector load impedance is the same for single-output and differential configuration. The conventional differential configuration uses two photodetectors, which gives lower optical power per detector than this delayed differential method, but at the expense of twice the total capacitance from the two detectors. The same optical power per unit area can be realized in this delayed differential configuration by doubling the detector area, which also doubles the detector capacitance. For narrow-band applications, the link gain reduction due to detector capacitance can be removed from either configuration by reactive matching if the parasitic series resistance of the detectors is sufficiently small.

The effective RIN gain $G_{\rm RIN}$, which was defined earlier in (3), is zero for perfect amplitude and phase balance between the channels. The results derived here for the delayed differential configuration are valid, in general, for conventional differential links and for differential links which use optical attenuation to balance the two channels and cancel RIN, except that for the delayed differential configuration, $G_{\rm RIN}$ is also limited by the operating bandwidth.

The noise figure of a differential link relative to the shot-noise limit for a single-output link at quadrature is shown in Fig. 4(a) as a function of modulator-bias angle, where the differential summing of the signals is assumed to be lossless. The optimum differential noise figure is plotted in Fig. 4(b). In order to cancel laser RIN, the output with more optical power needs to be attenuated, which also attenuates the modulation signal. Consequently, the differential method has a more rapid decrease in signal gain as the modulator is biased away from quadrature, compared to a single-output modulator where the signal gain changes relatively slowly as a function of bias angle. For a differential link with sufficiently large RIN cancellation, the optimum noise figure $F_{\rm quad2}$ at quadrature is

$$F_{\rm quad2} = 1 + F_{q,\,\rm shot}\left(\frac{1}{2} + \frac{p_{\rm amp}}{4} + G_{\rm RIN}p_{\rm RIN} \right). \tag{27}$$

$$\rm SFDR_1 = \left(\frac{2I_q}{qB} \cdot \frac{\sin^2\theta}{1+\cos\theta+p_{\rm amp}+p_{\rm RIN}(1+\cos\theta)^2+p_{\rm mod}\sin^2\theta} \right)^{2/3} \tag{22}$$

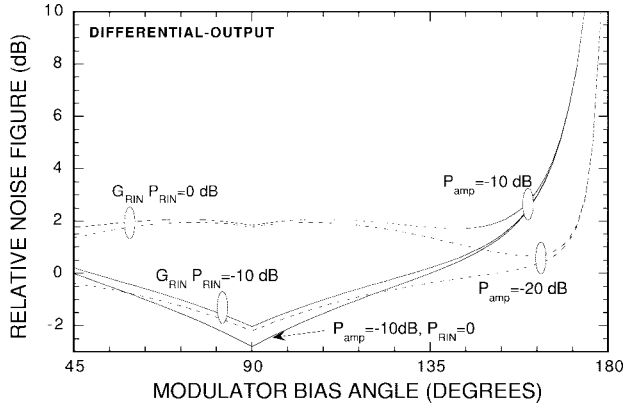

(a)

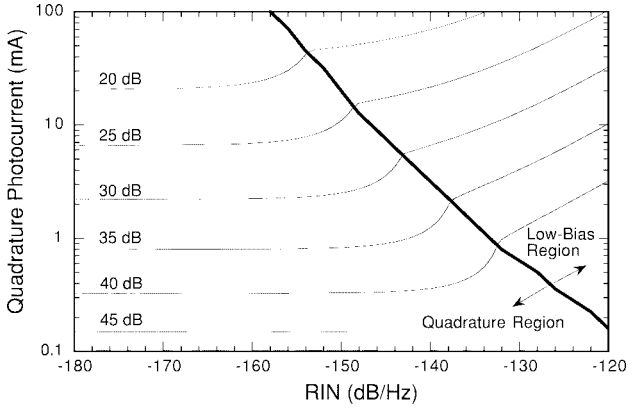

(b)

Fig. 4. (a) Optimum noise figure of a differential link relative to the shot-noise limit of a single-output link at quadrature as a function of modulator bias-angle using normalized parameters. (b) Noise figure of a differential link as a function of RIN and photocurrent for $G_{\rm RIN} = -20$ dB, $V_\pi = 5$ V, $R_s = 50\ \Omega$, $R_d = 50\ \Omega$, $F_a = 2$ dB.

For sufficiently low laser RIN and amplifier noise, the optimum differential noise figure $F_{\rm quad2} \cong F_{q,\,\rm shot}/2$ is the same as the optimum single-output noise figure $F_{\rm opt1}$, but a comparison of (15) and (27) shows that the differential method can maintain this optimum performance for a higher level of laser RIN if $G_{\rm RIN}$ is sufficiently small, and also for a higher level of amplifier noise resulting from low optical power. The quadrature-biased differential link also has considerably higher gain than the low-biased single-output modulator because it is operated at the bias point for maximum gain and because both modulator output signals are used. In practice, the polarization combiner used in the delayed differential method contributes some insertion loss, which degrades both gain and dynamic range, although this insertion loss can be <0.5 dB and is neglected here.

Low modulator bias also can be used to reduce the effect of RIN for differential links with imperfect RIN cancellation, just as it does for single-ended links. The differential noise

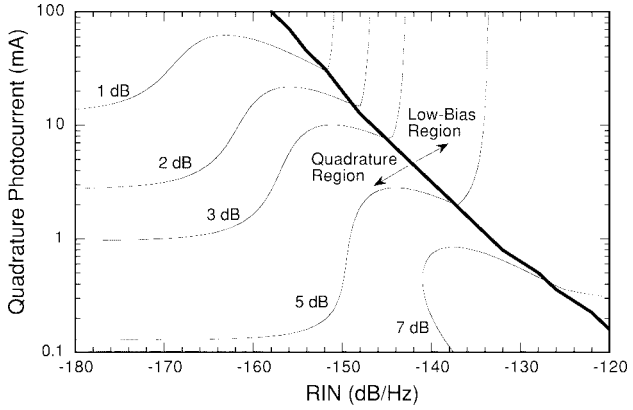

Fig. 5. Noise-figure improvement for a differential link compared to an identical low-biased single-ended link for RIN cancellation factor $G_{\rm RIN} = -20$ dB, $R_d = 50\ \Omega$, $F_a = 2$ dB.

figure $F_{\rm opt2}$ at low bias for small $p_{\rm amp}$ is approximately

$$F_{\rm opt2} \cong 1 + F_{q,\,\rm shot}\left(1 - \frac{p_{\rm amp}}{2} + \sqrt{p_{\rm amp}}\sqrt{4G_{\rm RIN}p_{\rm RIN} - 1}\right). \tag{28}$$

The optimum noise figure is given by the smaller of $F_{\rm quad2}$ and $F_{\rm opt2}$. By comparing (27) and (28), it can be seen that for small $p_{\rm amp}$ and $p_{\rm RIN}$, the differential noise figure at low-bias $F_{\rm opt2}$ is approximately twice as high as the noise figure at quadrature $F_{\rm quad2}$ because there is twice as much shot noise due to the two channels, but not substantially more modulation signal. Under these conditions of small $p_{\rm amp}$ and $p_{\rm RIN}$, the optimum modulator bias would be at quadrature.

The improvement in noise figure for a differential link compared to an otherwise identical single-output link in the high V_π limit is shown in Fig. 5 as a function of laser RIN and photocurrent. This noise-figure difference does not depend on the value of V_π or source impedance R_s. The differential configuration has better performance over the full calculation range, although the improvement is smallest at high optical power and low laser RIN. For small $p_{\rm amp}$, the boundary between optimum bias being at quadrature or being at a low bias is the condition $G_{\rm RIN} * p_{\rm RIN} = 1/2$. As $p_{\rm amp}$ increases, this optimum bias-point boundary moves to higher values of $G_{\rm RIN} * p_{\rm RIN}$. Better RIN suppression gives lower $G_{\rm RIN}$, and higher laser RIN can be tolerated before low modulator bias becomes optimum for the differential configuration.

The differential-link spurious-free dynamic range $\rm SFDR_2$ where the stronger optical output is optically attenuated to cancel the RIN contribution is shown in (29), at the bottom of this page.

The dynamic range is maximum at the bias where the noise figure is a minimum [10]. If the laser RIN is sufficiently suppressed by differential detection then the optimum bias occurs at quadrature and the dynamic range $\rm SFDR_{quad2}$ in

$$\mathrm{SFDR}_2 = \left(\frac{8I_q}{qB} \cdot \frac{(1 - |\cos\theta|)}{2\sin^2\theta + p_{\rm amp}(1 + |\cos\theta|) + 4(1 - |\cos\theta|)(G_{\rm RIN}p_{\rm RIN}\sin^2\theta + p_{\rm mod})}\right)^{2/3} \tag{29}$$

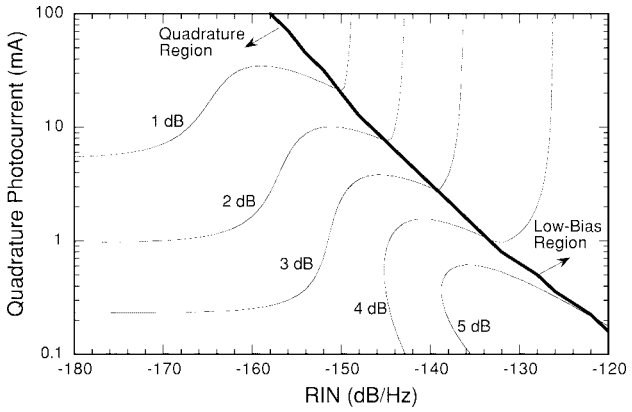

Fig. 6. Dynamic-range improvement for a differential link compared to an identical low-biased single-ended link for RIN cancellation factor $G_{\rm RIN} = -20$ dB, $R_d = 50\ \Omega$, $F_a = 2$ dB.

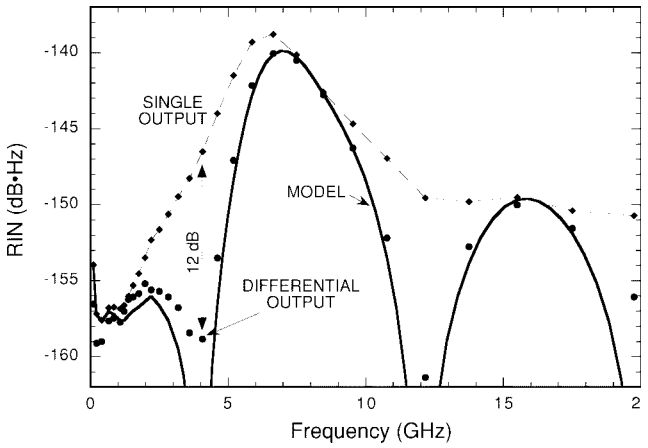

Fig. 7. Measured and calculated RIN as a function of frequency for the DFB laser with a fiber delay set for noise cancellation at 4 GHz for measured single-output noise, measured delayed differential RIN, and calculated delayed differential RIN.

the high V_π limit is

$$\mathrm{SFDR}_{\rm quad2} \cong \left(\frac{4I_q}{qB(1+p_{\rm amp}/2+2G_{\rm RIN}p_{\rm RIN})}\right)^{2/3}. \quad (30)$$

This optimum differential dynamic range $\mathrm{SFDR}_{\rm quad2}$ is equal to the optimum single-output dynamic range $\mathrm{SFDR}_{\rm opt1}$ for small $p_{\rm RIN}$ and $p_{\rm amp}$, although the differential method can maintain this optimum performance with higher levels of laser RIN and amplifier noise.

If the product $G_{\rm RIN} * p_{\rm RIN}$ is large, then the optimum bias point occurs at low modulator bias. The optimum dynamic range $\mathrm{SFDR}_{\rm opt2,\,shot}$ in the high V_π limit for small $p_{\rm amp}$ is approximately

$$\mathrm{SFDR}_{\rm opt2,\,shot} \cong \left(\frac{2I_q}{qB\left(1-p_{\rm amp}/2+\sqrt{p_{\rm amp}}\sqrt{4G_{\rm RIN}p_{\rm RIN}-1}\right)}\right)^{2/3}. \quad (31)$$

The improvement in spurious-free dynamic range for a differential link and an otherwise identical single-output link is shown in Fig. 6, where the same trends can be seen as for the improvement in noise figure.

V. Experiment

An optical link was implemented with the configuration shown in Fig. 1(c) using a distributed feedback (DFB) diode laser and an $LiNbO_3$ dual-output modulator from UTP with a V_π of $\sim$5 V at dc. The measured half-wave voltage V_π of the modulator was 6.9 V at 4 GHz. The two outputs were combined in a polarization coupler with a fiber delay of 180° at an RF frequency of 4.01 GHz.

The laser RIN, shown in Fig. 7, was measured after the modulator at a laser bias current of 117 mA. The single modulator output RIN is the actual RIN of the laser, while the RIN measured using the delayed differential configuration is modified by $G_{\rm RIN}$. Also shown is the apparent RIN expected for a delayed differential configuration, calculated from the measured laser RIN and theoretical RIN gain. For these calculations, measured values of V_π are used, which vary from 6.1 V at 3 GHz to 8.2 V at 5 GHz.

The theoretical response has infinite RIN suppression for perfect amplitude balance between the two modulator outputs. However, an experimental RIN suppression limit was observed. The largest RIN suppression for the differential output configuration plotted in Fig. 7 was approximately 12 dB, although up to 17 dB has been observed. This noise-suppression limit is believed to be due to imperfect polarization isolation in the polarization coupler. Although the polarization combiner acts principally as an incoherent combiner, imperfect polarization isolation between the modulator outputs causes a second parasitic Mach–Zehnder interferometer. Due to the large delay in one arm of this interferometer, it acts as a highly sensitive converter of optical frequency-modulation noise to amplitude-modulation noise. This noise-reduction technique was found to be unsuitable for low-frequency links because the interferometer effect is larger for the larger difference in the optical path length.

There are a number of ways to reduce the effect of this interferometric noise on the system. One method is to modulate the laser with an out-of-band signal to introduce laser chirp and destroy the coherent interaction. This method has been used to reduce interferometric interactions due to multiple optical reflections in the link [19], [20]. Another way to minimize the effect of this undesired interferometer would be to actively control the optical phases in this second interferometer in order to minimize the conversion of frequency-modulation noise to amplitude-modulation noise. These optical phases could be set by injecting a pilot tone into the laser at an odd multiple of the noise-cancellation frequency, and adjusting the optical phase in the second Mach–Zehnder interferometer to null this modulation signal at the output.

The experimental link gain and noise figure are shown as a function of modulator-bias angle in Fig. 8 for a peak photocurrent from each modulator output of 1.8 mA. The

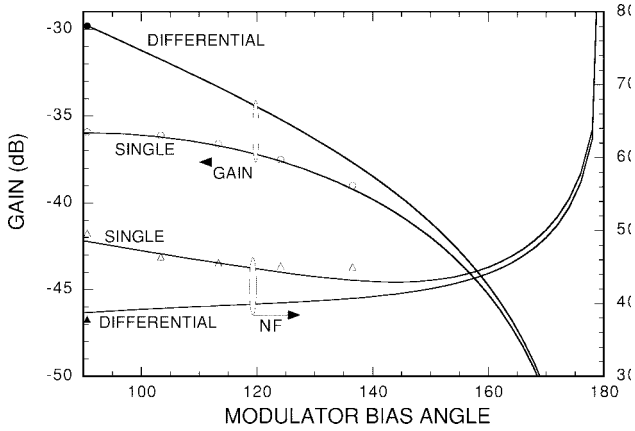

Fig. 8. Measured and calculated gain and noise figure as a function of bias angle at a modulation frequency of 4 GHz.

link results include the 0.5 dB of optical splitting loss of the polarization combiner, which does not substantially affect the noise figure or dynamic range of the link. The measured data agrees well with the model. The optimum noise figure of the single-output link occurs at low modulator bias in order to minimize the effect of laser RIN. The optimum noise figure of the differential-output link occurs at quadrature bias where the link gain was a maximum.

VI. Summary

A new method of narrow-band laser RIN cancellation in external-modulation optical links, which uses the two complementary outputs of a Mach–Zehnder interferometer, is proposed and demonstrated. One modulator output is delayed 180° of the RF modulation period with respect to the other to cancel the amplitude noise while enhancing the modulation signal. This cancellation occurs over a narrow frequency bandwidth and, in theory, can give 20 dB of RIN cancellation over a ∼13% relative bandwidth. For ideal incoherent addition of the two modulator outputs, this method gives the same noise and signal performance at the center of the RF band as for a conventional differential link, but without the tight tolerance on fiber length matching over a long distance. This delayed differential method is particularly well suited for high-frequency applications using semiconductor laser sources where resonance-enhanced intensity noise degrades performance. Monolithic implementation becomes more feasible as the modulation frequency increases, and should be practical for millimeter-wave applications.

The relative performance of differential links and single-ended links is analyzed using a set of normalized parameters, where the relative performance of many links can be analyzed using one or two parameters. Analytic expressions for gain, noise figure, and dynamic range are derived for low-biased and differential links. For wide-band links, the modulator must be biased at quadrature in order to minimize second-order distortion, and the differential method substantially improves performance. For narrow-band links, the effect of RIN can be substantially reduced by low biasing the modulator, and the improvement using a differential link is smaller.

In this paper, it is shown for narrow-band links that low modulator bias can also be used with the differential method by optically or electrically attenuating one modulator output to balance the RIN contribution from each channel. The performance at low bias using optical attenuation is poorer than if a low RIN laser source is used, as the attenuated output adds shot noise without substantially increasing the modulation signal. However, the low-biased differential links are considerable less sensitive to reduction in RIN suppression caused by amplitude and phase balance between the two outputs than quadrature-biased differential links. As a result, low modulator bias could be used to increase the effective operating bandwidth of delayed differential links.

A delayed differential optical link was demonstrated at 4 GHz using a DFB diode pump laser and a broad-band $LiNbO_3$ modulator. The resulting link performance was compared to the standard link configuration by using only one output of the modulator. Using both outputs of the modulator reduced the link noise figure by ∼5 dB. RIN suppression is believed to be limited by FM–AM conversion due to imperfect optical summing, which could be reduced by reducing the coherent optical interaction.

Acknowledgment

The author greatly appreciates the assistance of E. Ackerman, M. Corcoran, C. Cox, H. Roussell, M. Taylor, J. Vivilecchia, and A. Yee.

References

[1] T. S. Chu and M. J. Gans, "Fiber optic microcellular radio," *IEEE Trans. Veh. Technol.*, vol. 40, pp. 599–606, Aug. 1991.
[2] B. D. Carlson, L. M. Goodman, J. Austin, M. W. Ganz, and L. O. Upton, "An ultralow-sidelobe adaptive array antenna," *Lincoln Lab. J.*, vol. 3, pp. 291–309, 1990.
[3] B. Oliver, "Signal-to-noise ratios in photoelectric mixing," *Proc. IRE*, vol. 49, pp. 1960–1961, 1961.
[4] H. van de Stadt, "Heterodyne detection at a wavelength of 3.39 μm for astronomical purposes," *Astron. Astrophys.*, vol. 36, pp. 341–348, 1974.
[5] S. Yamashita and T. Okoshi, "Suppression of common-mode beat noise from optical amplifiers using a balanced receiver," *Electron. Lett.*, vol. 28, pp. 21–23, 1992.
[6] E. Ackerman, S. Wanuga, J. MacDonald, and J. Prince, "Balanced receiver external modulation fiber-optic link architecture with reduced noise figure," in *IEEE MTT-S Symp. Dig.*, vol. 2, Atlanta, GA, 1993, pp. 615–618.
[7] K. J. Williams and R. D. Esman, "Optically amplified downconverting link with shot-noise-limited performance," *IEEE Photon. Technol. Lett.*, vol. 8, pp. 148–150, Jan. 1996.
[8] C. Cox, E. Ackerman, R. Helkey, and G. Betts, "Techniques and performance of intensity-modulation direct-detection analog optical links," *IEEE Trans. Microwave Theory Tech.*, vol. 45, pp. 1375–1383, Aug. 1997.
[9] B. H. Kolner and D. M. Bloom, "Electrooptic sampling in GaAs integrated circuits," *IEEE J. Quantum Electron.*, vol. QE-22, pp. 79–93, Jan. 1986.
[10] E. Ackerman, S. Wanuga, D. Kasemset, A. S. Daryoush, and N. R. Samant, "Maximum dynamic range operation of a microwave external-modulation fiber-optic link," *IEEE Trans. Microwave Theory Tech.*, vol. 41, pp. 1299–1306, Aug. 1993.
[11] M. L. Farwell, W. S. C. Chang, and D. R. Huber, "Increased linear dynamic range by low biasing the Mach–Zehnder modulator," *IEEE Photon. Technol. Lett.*, vol. 5, pp. 779–782, July 1993.
[12] C. Cox, G. Betts, and L. Johnson, "An analytic and experimental comparison of direct and external modulation in analog fiber-optic links," *IEEE Trans. Microwave Theory Tech.*, vol. 38, pp. 501–509, May 1990.

[13] G. Betts, L. Johnson, and C. Cox, "Optimization of externally modulated analog optical links," *Proc. SPIE*, vol. 1562, pp. 281–302, 1991.
[14] B. H. Kolner and D. W. Dolfi, "Intermodulation distortion and compression in an integrated electrooptic modulator," *Appl. Opt.*, vol. 26, pp. 3676–3680, 1987.
[15] R. Helkey, J. Twichell, and C. Cox, "A down-conversion optical link with RF gain," *J. Lightwave Technol.*, vol. 15, pp. 956–961, June 1997.
[16] H. Skeie and R. V. Johnson, "Linearization of electro-optic modulators by a cascade coupling of phase modulation electrodes," in *SPIE Proc. Integrated Opt. Circuits*, vol. 1583, Boston, MA, 1991, pp. 153–164.
[17] W. K. Burns, "Linearized optical modulator with fifth order correction," *J. Lightwave Technol.*, vol. 13, pp. 1724–1727, Aug. 1995.
[18] J. F. Lam and G. L. Tangonan, "A novel optical modulator system with enhanced linearization properties," *IEEE Photon. Technol. Lett.*, vol. 3, pp. 1102–1104, Dec. 1991.
[19] G. C. Wilson, T. H. Wood, J. L. Zyskind, J. W. Sulhoff, J. E. Johnson, T. Tanbun-Ek, and P. A. Morton, "SBS and MPI suppression in analogue systems with integrated electroabsorption modulator/DFB laser transmitters," *Electron. Lett.*, vol. 32, pp. 1502–1504, 1996.
[20] R. Helkey and H. Roussell, "Delayed differential RIN reduction with interferometric noise suppression," in *Opt. Fiber Commun. Conf.*, San Jose, CA, Feb. 1998, pp. 259–260.

Roger Helkey (M'88) received the B.S. degree in engineering with honors from the California Institute of Technology, Pasadena, in 1982, and the M.S. and Ph.D. degrees in electrical engineering from the University of California at Santa Barbara, in 1988 and 1993.

Since 1995, he has been a Staff Member at the MIT Lincoln Laboratory, Lexington, where he works on high-dynamic-range analog optical links. From 1983 to 1995, he was a Researcher at the University of Tokyo, and at Advanced Telecommunications Research, Japan, where he studied microcavity effects and nonlinear optical switching. From 1984 to 1986, he was a Microwave Engineer at Watkins–Johnson. From 1982 to 1984, he was a Project Design Engineer at Trimble Navigation. He has designed RF, microwave, and optical filters, microwave amplifiers, switches, and subsystems, oscillators, phased-locked loops, and CMOS, bipolar, and GaAs integrated circuits. He has constructed novel mode-locking structures for optical pulse generation, optical sampling systems, frequency-conversion links with gain, and direct and external analog optical links using new intensity noise-reduction techniques. He has developed analytic and numerical methods for a variety of optical design problems. He has coauthored a book chapter and holds a number of patents.